Letters in Applied NanoBioScience
Open-Access Journal (ISSN: 2284-6808)

Article
Volume 12, Issue 2, 2023, 41
https://doi.org/10.33263/LIANBS122.041

Synthesis and Spectral Characterization of Novel Schiff Base and Fe(II) Complex: Evaluation of Antibacterial, Antifungal, and Anticancer Properties

Mukkanti Siva Naga Anjaneya Prasad [1], Reddy Prasad Puthalapattu [1], Bonnige Kishore Babu [2], Suvardhan Kanchi [3,4,*]

[1] Department of Chemistry, Institute of Aeronautical Engineering, Dundigal, Hyderabad, Telangana, India
[2] Department of Engineering Chemistry, AU College of Engineering, Andhra University, Visakhapatnam, A.P., India; prprasadchem@gmail.com (R.P.P.);
[3] Department of Chemistry, Sambhram Institute of Technology, M.S. Palya, Jalahalli East, Bengaluru 560097, India; ksuvardhan@gmail.com (S.K.);
[4] Department of Chemistry, Sambhram University, Khamraqul Street, Jizzakh City 130100, Republic of Uzbekistan
* Correspondence: ksuvardhan@gmail.com (S.K.); prasad.mukkantis@gmail.com (M.S.N.A.P.);

Scopus Author ID 36699599700
Received: 10.12.2021; Accepted: 5.01.2022; Published: 17.03.2022

Abstract: Schiff's bases are a type of molecule found in medical chemistry that has been shown to have substantial antibacterial and chemotherapeutic properties. On the other hand, Ortho phenylenediamine is a broad category of synthetic chemical with various pharmacological properties, including anticancer potential. Their antibacterial, antifungal, and anticancer properties, in particular, make the compounds appealing for future derivatization and screening as potential therapeutic agents. Accordingly, this study aimed to synthesize a novel Schiff's base-Fe(II) complex using the self-assembly method for in-vitro studies due to its potential drug properties for therapeutic intervention in various diseases. The as-synthesized Fe(II) complex was characterized by spectral and elemental techniques. The obtained data from the elemental analysis was in good agreement with the general formula MLCln (L= Ligand complexed with Fe(II) via carbonyl group, the nitrogen of hydrazine group, and oxygen). Additionally, Fe(II) complexes with Schiff's bases were shown to have gastro-protective, antiproliferative, and antibacterial properties. The Schiff's base and its Fe(II) complex were screened against gram-positive *(B.subtilies*), gram-negative (*E.coli*) as well as *A.niger* to evaluate the antibacterial and antifungal properties, respectively. The obtained results demonstrated that the Schiff's base –Fe(II) complex has higher antibacterial and antifungal activity than Schiff's base ligand. Furthermore, cytotoxicity studies were performed for Schiff base and its Fe(II) complex against breast cancer (MCF-7) cell lines. The findings of this study recommended new insights in the field of medicine to consider Schiff's base-Fe(II) complex as a potential candidate for the antibacterial, antifungal, and anticancer agent.

Keywords: Schiff's base; Fe(II); antibacterial; antifungal and anticancer agent.

1. Introduction

Macrocyclic transition metal complexes have gained the attention of researchers for their effective antifungal, antibacterial and anticancer properties, making the compounds appealing for future derivatization and screening as potential therapeutic agents [1-5]. These complexes can undergo tetra-dentate chelation with heavy metal ions, bonding through nitrogen and Sulphur, largely responsible for their biological actions [6,7]. Since it was

discovered that several of these organic metal complexes could serve as facsimiles for biologically relevant entities, the study of coordination chemistry has gained interest in Schiff base and their complexes [8,9]. Due to their significance as synthetic models for iron-containing enzymes [10,11,12], oxidized catalysts [13,14], and stable materials depending on the pressure, temperature as well as spin-crossover due to light [15,16], the modeling, synthesis, and interpretation of Fe(II) complexes with Schiff base ligands play a vital role in the iron-related coordination chemistry concepts. Schiff base ligands are preferred ligands since they are easily made by combining an aldehyde and primary amines in an alcohol solvent in a single pot [10].

Furthermore, it was recognized that some Fe(III) complexes serve as geometric and functional models for the heme-iron 'enzymes' identically complexed Fe(III) sites [17]. Several studies [18,19] have demonstrated that the investigation of structural properties of organic Fe(III) metal complexes with amidantate ligands resulted in the modeling of Bleomycin [20], and antitumor drug. The Fe (III) complexes with salicylidene amine ligands include a better structural and functional analog for the identically coordinated Fe(III) sites observed in hemi iron enzymes from a bioinorganic perspective [21]. During the current work, Schiff's base of Fe(II) complex was tried to improve the activities, contributing to a better avenue of investigation focusing on the potential of iron-based inorganic medicine. Because different ligands exhibit varied biological capabilities despite having slightly different molecular structures, their activities have been discovered to be highly reliant on the type of the metal ion and the donor atoms of the ligands.

This study synthesized a novel Schiff base and its Fe(II) complex using the self-assembly method. The as-synthesized ligand and organic metal complex were examined for antibacterial, antifungal, and anticancer properties against gram-positive (*B.subtilies*), gram-negative (*E.coli*), and *A.niger*. Additionally, cytotoxicity studies against breast cancer (MCF-7) cell lines were also conducted to confirm the potentiality of these materials in the field of medicine for prospects. To the best of our knowledge, this is the first report on the synthesis of 5, 10, 15, 20-tetrakis (para-x phenyl)porphyrinato and Fe(II) complex for the assessment of antimicrobial and anticancer properties. The results showed that Fe(II) porphyrins containing -COOH had the best antibacterial action, which might be due to the -COOH 'group's strong binding capacity to many biological molecules and its permeability.

2. Materials and Methods

2.1. Chemicals and reagents.

Chemical reagents of analytical reagent grade were used. All compounds such as ferrous sulphate sulfate, dimethyl sulfoxide, methanol, sodium azide, salicylaldehyde, acetone, and dimethylformamide were utilized in this investigation were obtained from Merck, BDH, and Aldrich, India.

2.2. Instrumentation.

The Shimadzu spectrophotometer was used to record FTIR spectra with KBr pellet in the range of 4000 – 400 cm^{-1}. The spectrum in ethanol was measured with a Shimadzu UV-visible spectrophotometer in the range of 200-800 nm using 1 cm quartz cell length. The SMP30 Electrothermal Stuart apparatus was used to calculate melting points. The electrical

conductivity of the complex was measured using a WTW Inolabcond 720 digital conductivity meter at 25°C for 10^{-3} mol l^{-1} solution in dimethyl sulfoxide (DMSO) samples. Agilent mass spectrometer 5975 quadrupole analyzer was used to record mass spectra.

In DMSO and Bruner DRX, 1H and 13C NMR spectra were computed using a DRX (500-MHz) spectrometer (500-MHz). The compound shifts were measured in ppm concerning interior Me_4Si. The Euro Vectro-3000A was used to perform fundamental microanalyses of the ligand and its complexity.

The solutions and materials employed in the experiments related to antimicrobial studies were sterilized using autoclaves obtained from Gallen Kamp, The United Kingdom. Memmert Incubator was used to incubate the cultured bacteria dishes. The atomic absorption method was used to determine the concentration of metals present in the complex using an Analytic Jena (AA350) Atomic Absorption Spectrophotometer. The Gouy approach and the Johnson Mattey Catalytic system were used to find magnetic susceptibility magnitudes at room temperature. The thin-layer chromatography (TLC) was performed on aluminum plates covered with silica gel (Fluka) and iodine to preliminary confirm the synthesis of ligand and complex.

2.3. Synthesis of $[(Fe)(SAL)_2(OPD)_2(AA)_2(N_3)_2].(SO_4)_2(H_2O)_4\ CH_3OH$.

0.5 mmol of Schiff's base (0.156 g) was dissolved in 10 ml of hot methanol followed by adding 0.5 mmol of Ferrous sulfate (0.139 g) solution and 10 ml of deionized distilled water in a 25 ml beaker. The sudden appearance of dark green colored solution was observed. To this solution, 0.5 mmol of sodium azide (0.032 g) was added to 10 ml of deionized distilled water, resulting in teak brown colored precipitate forming after constant stirring for one hour at room temperature. The structural and elemental composition was as follows: $C_{40}H_{39}N_{10}FeO_2$(M.Wt.747.65), C=64.26; H= 5.26; N= 18.73. Found: C=63.88; H=4.98; N=17.39. The observed significant FTIR absorptions peaks (KBr disk, cm^{-1}): 3728, 3430, 2313, 1728, 1759, 1612, 1276, 1250, 1252, 905 cm^{-1}. The mass peaks (m/z): 209, 147, 342, 482, 599, 704, 929. From this reaction procedure, the obtained yield was about 0.186 g (56%).

2.4. Scheme of the synthetic route and proposed structure of the complex.

In this study, mononuclear complex of $[(Fe)(SAL)_2(OPD)_2(AA)_2\ (H_2O)_2].H_2O.(SO4)_2$ was successfully synthesized. Two deprotonated salicylaldehyde and the neighboring two oxygens of acetylacetone, two aqua ligands in the active center and six water molecules, two sulfate ions in the outer sphere make up the octahedral geometry of the Fe(II) complex, as shown in Figure 1.

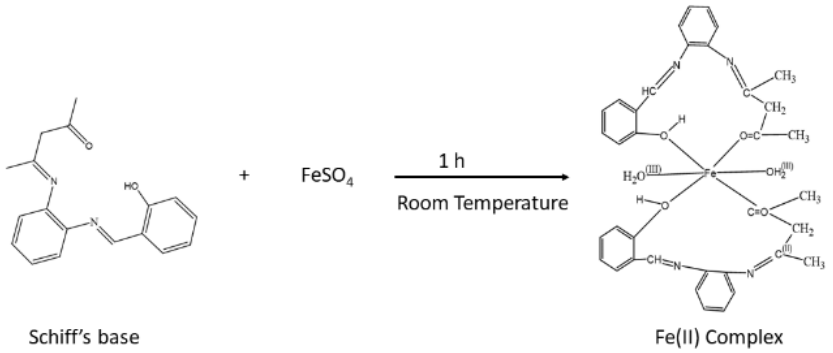

Figure 1. Schematic representation of reaction of Schiff's base with FeSO4 to form Fe(II) complex at required reaction conditions.

3. Results and Discussion

3.1. Spectrophotometric characterization of [(Fe)(SAL)$_2$(OPD)$_2$(AA)$_2$(N$_3$)$_2$]. (SO$_4$)$_2$(H$_2$O)$_4$ CH$_3$OH.

The UV-visible spectrophotometric absorption spectra of Schiff's base-Fe(II) complex were recorded in the range of 200 – 800 nm in dimethylformamide (DMF) medium. The results obtained demonstrate that the three absorption bands at 240 nm, 350 nm, and 450 nm were due to the characteristic transitions of π-π* and n-π* in the case of free Schiff's base, whereas in the Schiff's base-Fe(II) complex, these bands shifted to the longer wavelength with higher intensity. This behavior could be due to the donation of lone pair of electrons from the oxygen atom of Schiff's base to Fe(II) ion. In the case of Schiff's base –Fe(II) complex, three broad bands in the range of 256 – 300 nm, 351 – 355 nm, and 478 – 498 nm were observed. Interestingly, it was perceived that the poorly resolved an intense broadband in the range of 351 – 355 nm might be allocated to ligand-to-metal charge transfer (LMCT) or metal-to-ligand charge-transfer (MLCT). The ligand-derived high-intensity band of 250 nm was assigned to an intra-ligand n-π*or π-π* transition [22]. The broad shoulder bands of 300-325 nm on the Schiff's base-Fe(II) complexes can be attributed to the d–d transition key peaks as depicted in Figure 2.

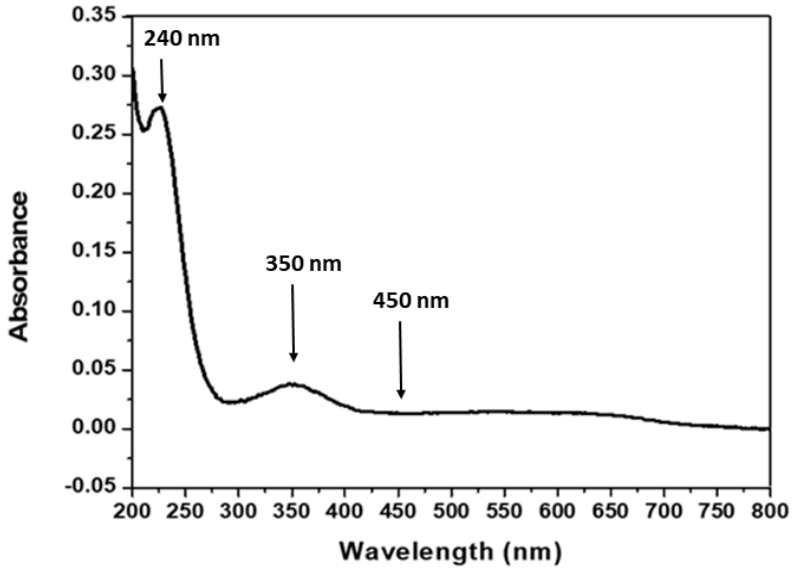

Figure 2. Electronic spectrum of [(Fe)(SAL)$_2$(OPD)$_2$(AA)$_2$ (H$_2$O)$_2$].H$_2$O.(SO$_4$)$_2$.

3.2. FTIR analysis.

3.2.1. Free Schiff's base [(Sal)(OPD)(AA)].

The ν(C=N) mode of the azomethine group was assigned to a sharp band found at 1612 cm-1 in the FTIR spectra of the free Schiff base ligand. In 3300-3500 cm^{-1}, the phenolic ν(O-H) mode was attributed to the hydroxyl group at the ortho position in the free Schiff's base ligand. The ligand also has a band at 1276 cm^{-1} due to the ν(C-O) phenolic group, as shown in Figure 3a.

3.2.2. [(Fe)(SAL)(OPD)(AA)].

Similar to free Schiff's base, a sharp band at 1612 cm^{-1} was assigned to the ν(C=N) mode of the azomethine group. It was noted that the lower shift in the wavenumber (1604–

1609 cm^{-1}) in a complex suggests the unanticipated nitrogen of azomethine with the metal centers.

The characteristic phenolic ν(O-H) mode due to a hydroxyl group at ortho position in the ligand was observed around 3200-3500 cm^{-1}. Due to the development of ν(M-O) bonds, a new band in the range of 500-543cm^{-1} appears in the Schiff's base –Fe(II) complex. The ν(C=O) of acetylacetone in the ligand was assigned to a sharp band detected at 1720 cm^{-1}. In the case of Schiff's base-Fe(II) complex, the strength of this band has somehow decreased but also shifted to lower wavenumbers, indicating that the carbonyl group is involved in metal ion complexation [22]. The presence of free sulfate ions in the outer sphere represents a week band at 1317cm^{-1}. The coordination of water with the Schiff's base-Fe(II) complex was evident in bands between 875 – 923 cm^{-1}, as shown in Figure 3b.

3.2.3. $[(Fe)(SAL)_2(OPD)_2(AA)_2\ (H_2O)_2].6H_2O.(SO_4)_2$.

In this study, a weak broadband was observed at 3419 cm-1, which contributes to the hydrogen-bonded –OH group. This shows that the Schiff 'bases' phenolic oxygen atoms were coordinated to the metal centers. When compared to free Schiff bases, the m(C=N) band, which occurs in the range of 1617– 1611 cm^{-1}, is somewhat displaced toward the lower wavenumber, showing the unanticipated nitrogen atom of azomethine with the metal center. The weak band at 2020 cm^{-1} suggests the presence of un-coordinated pseudo halide in the Schiff's base-Fe(II) complex, as shown in Figure 3c.

3.2.4. $[(Fe)(SAL)_2(OPD)_2(AA)_2(N_3)_2].(SO_4)_2(H_2O)_4\ CH_3OH$.

From FTIR spectrum, a sharp peak at 1612 cm^{-1} was assigned to the ν(C=N) mode of the azomethine group of Schiff bases ligand. The shift in the lower wavenumbers of the complex in the range of 1604–1609 cm^{-1} was mainly due to the unanticipated nitrogen atom of the azomethine with metal center [23]. In between 3200-3500 cm^{-1}, the phenolic ν(O-H) mode is found due to the presence of -OH at the ortho position of the ligand. Due to the formation of ν(M-O) bonds, a new band between 500-543 cm^{-1} appears in the complex [24]. The ν(C=O) of acetylacetone in ligands was ascribed to a narrow band detected at 1720 cm^{-1}. In the corresponding metal complexes, the strength of this band has somehow decreased but also shifted to lower vibrational modes, indicating that the carbonyl group was involved in metal ion complexation [25]. The presence of free sulfate ions in the outer sphere was indicated by the week band at 1317cm^{-1}. The existence of unanticipated methanol in the outer sphere was illustrated by the band at 2830 cm^{-1}. The presence of bands between 875-923cm^{-1} confirms the presence of chelated Fe(II) in the complex [26]. The hydrogen-bonded –OH group was evident from the weak and broad bands between 3746 – 3423 cm^{-1}. This demonstrates that the Schiff 'bases' oxygen atoms of the phenolic ring were coordinated to the metal centers. When compared to free Schiff's bases, the strong m(C=N) bands in the region of 1617–1611cm^{-1} were somewhat moved toward lower vibration at 1607 cm^{-1}, showing the unanticipated nitrogen atoms of azomethine with a metal center. The presence of an N-coordinated terminal azide group was suggested by the s(CN) absorption as a single peak at 2115 cm^{-1}.

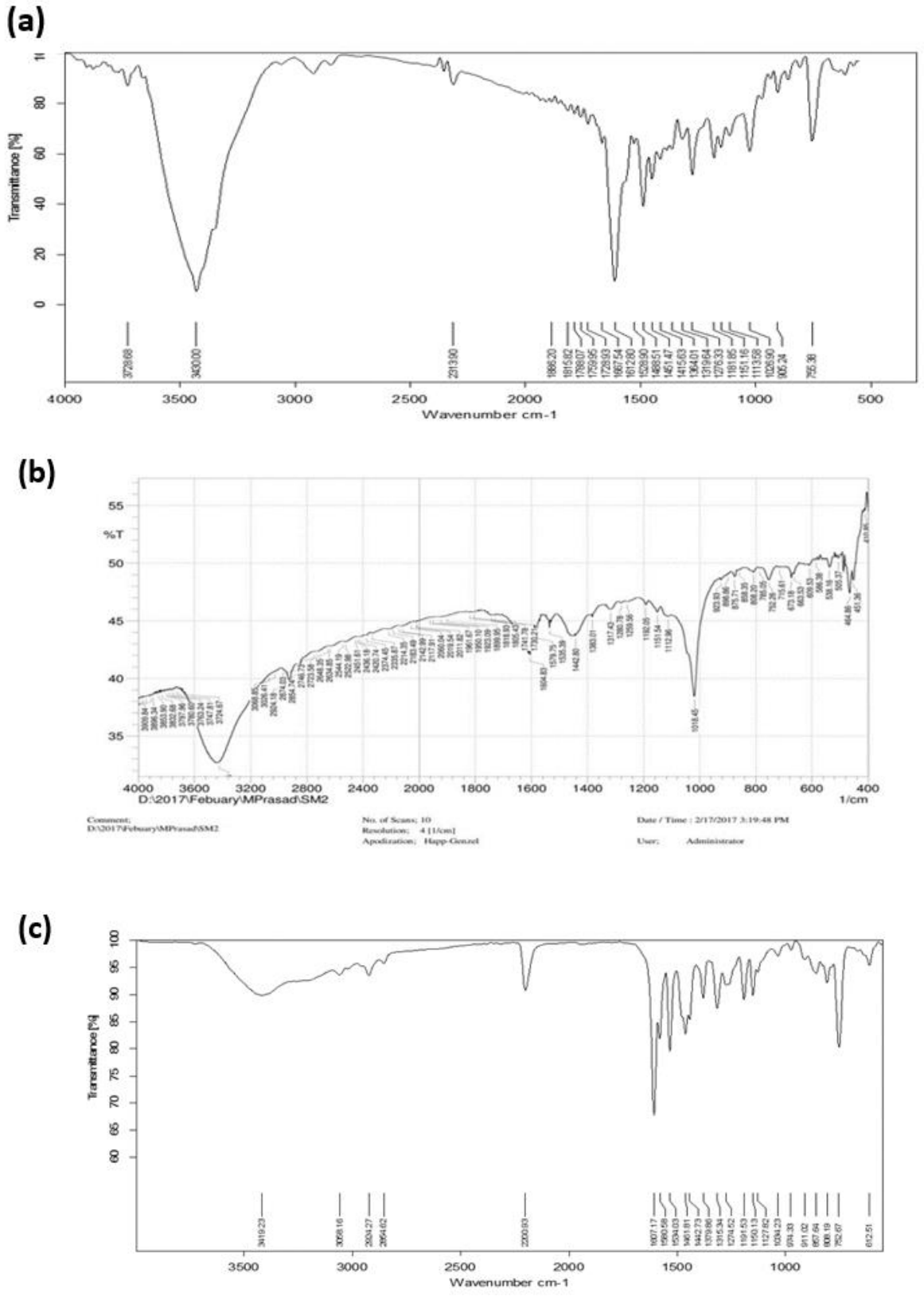

Figure 3. FTIR spectrum of (a) free Schiff's base [(Sal)(OPD)(AA)], (b) [(Fe)(SAL)(OPD)(AA)] and (c) $[(Fe)(SAL)_2(OPD)_2(AA)_2\ (H_2O)_2].6H_2O.(SO_4)_2$.

3.3. LC-MS characterization of free Schiff's base [(Sal)(OPD) (AA)] and $[(Fe)(SAL)_2(OPD)_2(AA)_2(N_3)_2].(SO_4)_2(H_2O)_4\ CH_3OH$.

Figure 4a shows two major peaks at 317 (m/z) and 211 (m/z), demonstrating that the complex has one salicylaldehyde, one acetylacetone, one OPD, one water molecule

[(SAL)(OPD)(AA)(H_2O)] and one salicylaldehyde, one OPD OPD [(SAL) (OPD)] respectively.

[(Fe)$(SAL)_2(OPD)_2(AA)_2(N_3)_2(CH_3OH)(SO_4)_2(H_2O)_4$] represents the complex attached to one Fe(II), two salicylaldehyde, two OPD, two acetylacetone, two azides, two sulfate, one methanol, and four water molecules due to the fragmentation observed at 929 (m/z). [$(SAL)_2(OPD)_2(AA)_2(OCH_3)$ (SO_4) $(H_2O)_2$] peak at 599 (m/z) shows complex allocated with two salicylaldehyde, two OPD, two acetylacetone, one methanol, one sulfate, two water fragments. The peak at 704 (m/z) of the complex reveals the presence of two salicylaldehyde, two OPD, two acetylacetone, one methanol, one sulfate, two water molecules as represented in [$(SAL)_2(OPD)_2(AA)_2(OCH_3)$ (SO_4) $(H_2O)_2$]. Whereas, the peat at 599 (m/z) indicates the complex embedded with two salicylaldehyde, two OPD, one acetylacetone, one sulfate, one methanol, and one water molecules as shown in [$(SAL)_2(OPD)_2(AA)$ $(SO_4)(CH_3OH)(H_2O)$]. The peak at 482 (m/z) demonstrates that the complex was bounded with two salicylaldehyde, one OPD, one acetylacetone, one sulfate, and one methanol as ascribed to [$(SAL)_2(OPD)(AA)(SO_4)(CH_3OH)$]. The complex with a peak at 342 (m/z) ensures one salicylaldehyde, one OPD, one acetylacetone, and one sulfate molecule as mentioned in [(SAL)(OPD)$(AA)(SO_4)$]. [(SAL)(OPD)] characterises the base peak at 209 (m/z), while [$(OPD)(N_3)$] denotes the peak at 147 (m/z). Figure 4b depicts fragmentation.

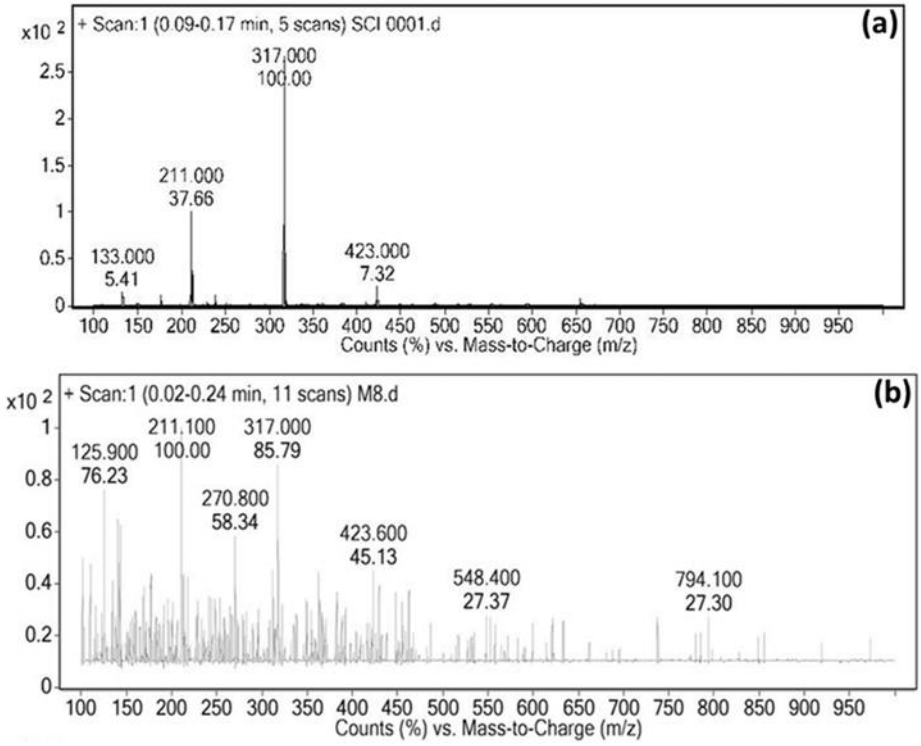

Figure 4. LC-MS Spectrum of (**a**) free Schiff's base [(Sal)(OPD) (AA)] and (b) [(Fe)$(SAL)_2(OPD)_2(AA)_2$ $(H_2O)_2$].H_2O.$(SO_4)_2$.

3.4. 1H-NMR Spectrum of [(Fe)$(SAL)_2(OPD)_2(AA)_2(N_3)_2$].$(SO_4)_2(H_2O)_4$ CH_3OH.

In dimethyl sulfoxide (DMSO) solution, the 1HNMR spectra of Schiff's bases were recorded with tetramethylsilane (TMS) as an internal standard. The Schiff's bases' NMR spectra and the spectra of the complexes were compared to those of the parent Schiff's bases. The N-CH signal, which occurred in the spectra of the ligand at 8.85-8.96 ppm, also appeared in the spectrum of its Fe(II) complex, confirming the presence of an azomethine group in the

complex. Furthermore, the signal at 2.5 ppm indicates the free methyl groups present in acetylacetone. Figure 5b shows a new signal at 3-3.5 ppm, which attributes to methanol's presence in the complex.

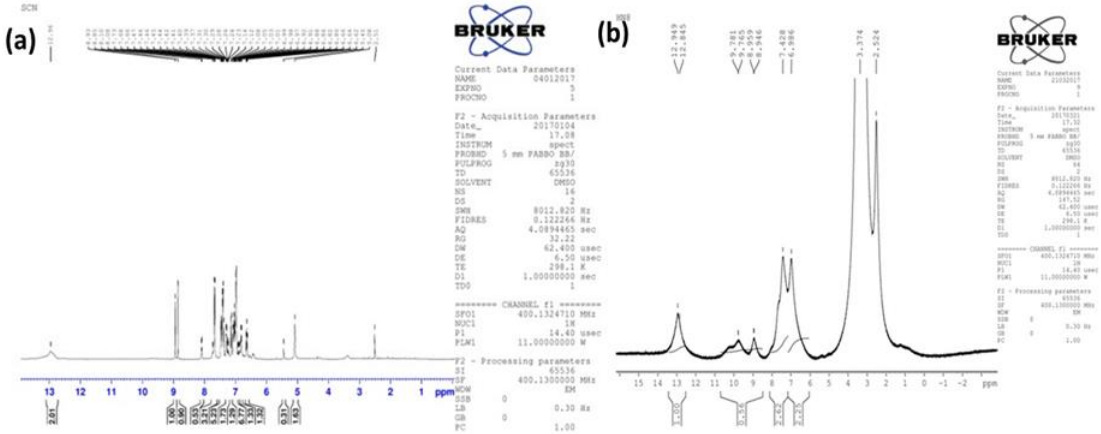

Figure 5 1H-NMR Spectrum of (a) free Schiff's Base (SAL)(OPD)(AA) and (b) $[(Fe)(SAL)_2(OPD)_2(AA)_2(H_2O)_2].H_2O.(SO_4)_2$.

3.5. Antimicrobial screening of Schiff's base and Fe(II) complex.

The as-synthesized free Schiff's base and its Fe(II) complex were evaluated for antibacterial against gram-negative, gram-positive bacteria, and antifungal activity using the Agar-well diffusion method [27-30]. The results obtained from this study were tabulated in Table 1.

Table 1. Antimicrobial activities of Schiff's base ligand and Fe(II) complex.

Schiff's base ligand	
Bacteria	**Inhibition zone (mm)**
Gram positive (*B.subtilis*)	8
Gram negative (*E.coli*)	8
Fungi	Inhibition zone (mm)
A.Niger	7
Schiff's base –Fe(II) complex	
Gram positive (*B.subtilis*)	12
Gram negative (*E.coli*)	16
Fungi	Inhibition zone (mm)
A.Niger	Nil

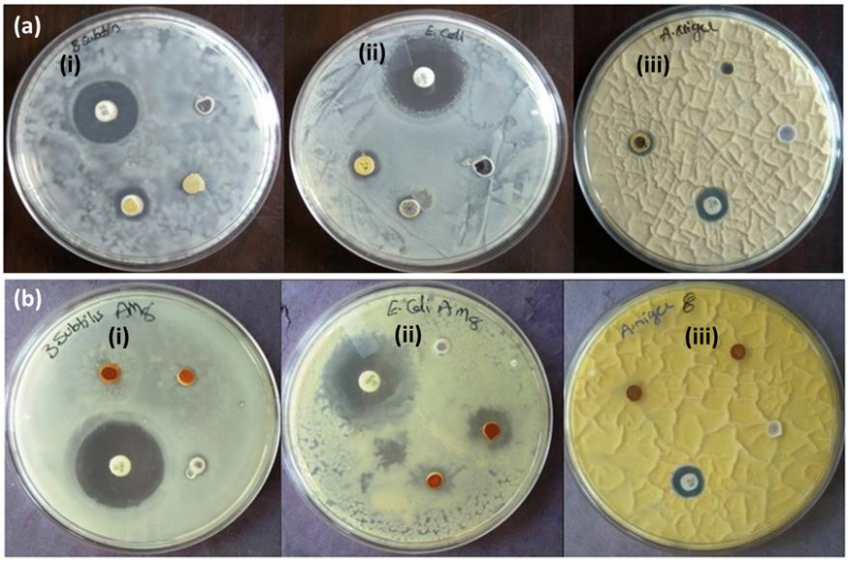

Figure 6. Antimicrobial activities of (a) free Schiff's base and (b) Schiff's base-Fe(II) complex by showing the inhibition zones against gram-positive, gram-negative bacteria and fungus.

From Figure 6a-b, it was clear that the antibacterial and antifungal activity was higher in the case of Schiff's base-Fe(II) complex than free Schiff's base ligand. The inhibition zones of antibacterial and antifungal for ligand were found to be 8 mm and 7 mm, whereas, in the case of Fe(II) complex, these values were doubled (Table 1). The obtained results demonstrate the potentiality of novel Schiff's base –Fe(II) complex against *B.subtilis* gram-positive) and *E.coli* (gram-negative) bacteria. In the case of *A.Niger* (fungus), the antifungal activity was higher than the antibacterial activity, as shown in Table 1. Therefore, it demonstrates that Schiff's base –Fe(II) complex is one of the promising candidates in the field of inorganic medicine.

3.6. Cytotoxic studies of $[(Fe)(SAL)_2(OPD)_2(AA)_2(N_3)_2].(SO_4)_2(H_2O)_4\ CH_3OH$.

The synthesized Schiff's base-Fe(II) complex was screened to evaluate the cytotoxicity properties against breast cancer (MCF-7) cell lines [31-63]. According to the findings, the complex demonstrated its cytotoxic properties as IC50 (g/mL) against breast cancer MCF-7 cell lines. From Figure 7, it was clear that the Fe(II) complex has a high capacity of killing as well as inhibiting the growth of the cancerous cells, similar to the literature report [64-66]. The IC_{50}values of the Schiff's base-Fe(II) complex were tabulated in Table 2. The obtained results clearly demonstrate that with the increase in the concentration of Schiff's base Fe(II) complex, the cell survival capacity decreases; thereby, inhibition capacity increases to 10 µg/mL. Beyond 10 µg/mL, the inhibition activity slightly decreases due to the attainment of saturation point.

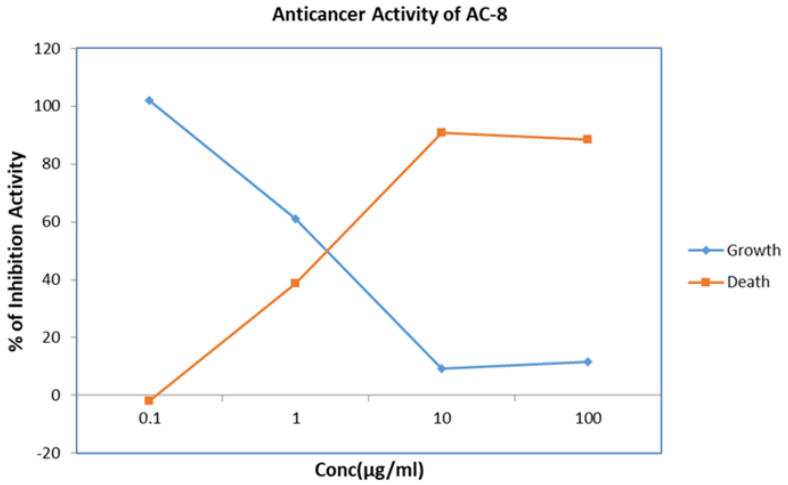

Figure 7. A plot showing the % of inhibition activity as a function of the concentration of Schiff's base-Fe(II) complex.

Table 2. IC_{50}values of the Schiff base-Fe(II) complex.

Concentration (µg/ml)	Cell survival (%)	Cell inhibition (%)
0.1	101.9687	-1.96866
1	61.18923	38.81077
10	9.321012	90.67899
100	11.65127	88.34873

4. Conclusions

This research created Schiff's base-Fe(II) pseudo halide ligand complex using the self-assembly method. To analyze the ligand as well as the complex, spectroscopic characterization techniques were applied. Antibacterial tests on the complex reveal an effective antibacterial agent, with MIC values of 12 and 16 for bacteria and no activity for fungal organisms. IC_{50}

values have been used to confirm the anticancer impact of the 'Schiff's base-Fe(II) complex in cytotoxic experiments against MCF-7 breast cancer cell lines.

Funding

This research received no external funding.

Acknowledgments

This research has no acknowledgment.

Conflicts of Interest

The authors declare no conflict of interest.

References

1. Kazem, B.; William, C.; Mohammad, H.H.; Ross, W.H.; Arash, L.; Morteza, M. Synthesis and crystal structure of the dinuclear copper(II) Schiff base complex l-hydroxido-lchlorido-bis{[bis(trans-2-nitrocinnamaldehyde)-ethylenediamine]chloridocopper(II)} dichloromethane sesquisolvate. *Acta Cryst* **2016**, *C72*, 239–242, https://doi.org/10.1107/S2053229616003144.
2. West, D.; Liberia, X.; Padhye, E.; Chikate, S.B.; Sonawane, R.C.; Kumar, P.B.; Yeranda, A.S. Thiosemicarbazone complexes of copper (II): structural and biological studies. *Coordination Chemistry Reviews* **1993**, *123*, 49-71, https://doi.org/10.1016/0010-8545(93)85052-6.
3. Canadas, M.; Torres, E.L.; Aris, A.M.; Mendrila, M.A.; Sevilla, M.T. Spectroscopic and electrochemical properties of nickel (II), iron (III) and cobalt (II) complexes with benzilbisthiosemicarbazone—importance of working conditions and the metal salt used in the final complex. *Polyhedron* **2000**, *19*, 2059-2068, https://doi.org/10.1016/S0277-5387(00)00505-2.
4. Kamal, S.T.A.J. Preparation, characterization, thermal studies, photochemical behaviours and antimicrobial activity of complexes derived from 5-Methyl-3-Furaldehyde Thiosemicarbazone and Hg(II) salts of hallo acids. *Bulletin of Pharmaceutical Sciences* **2010**, *33*, 95-105, https://doi.org/10.21608/bfsa.2010.147031.
5. Fox, O.D.; Cookson, J.; Wilkinson, E.J.S.; Drew, M.G.B.; MacLean, E.J.; Teat, S.J.; Beer, P.D. Nanosized polymetallic resorcinarene-based host assemblies that strongly bind fullerenes *Journal of the American Chemical Society* **2006**, *128*, 6990-7002, https://doi.org/10.1021/ja060982t.
6. Gamil, A.H.; Mohammed, S.S.; Ahmed, A.A. Ligand influence on the electrochemical behavior of some copper(II) thiosemicarbazone complexes. *Transition Metal Chemistry* **2005**, *30*, 464-470, https://doi.org/10.1007/s11243-005-2362-x.
7. Sun, L.; Liang, C.; Shirazian, S.; Zhou, Y.; Miller, T.; Cui, J.; Fukuda, J.Y.; Chu, J.Y.; Nematella, A.; Wang, X. Discovery of 5-[5-fluoro-2-oxo-1, 2-dihydroindol-(3 Z)-ylidenemethyl]-2, 4-dimethyl-1 H-pyrrole-3-carboxylic acid (2-diethylaminoethyl) amide, a novel tyrosine kinase inhibitor targeting vascular endothelial and platelet-derived growth factor receptor tyrosine kinase. *Journal of Medicinal Chemistry* **2003**, *46*, 1116-1119, https://doi.org/10.1021/jm0204183.
8. Ramesh, G.N.; Prathima, B.; Rao, Y.S.; Reddy, Y.P.; Pai, K.S.R.; Reddy, A.V. Synthesis, spectroscopic and antitumor studies on copper (II) complex of orthohydroxypropiophenone isonicotinoylhydrazone. *Arabian Journal of Chemistry* **2016**, *9*, S404-S410, https://doi.org/10.1016/ j.arabjc.2011.05.008.
9. Jayabalakrishnan, C.; Natarajan, K. Synthesis, characterization, and biological activities of ruthenium (II) carbonyl complexes containing bifunctional tridentate Schiff bases. *Synthesis and Reactivity in Inorganic and Metal-Organic Chemistry* **2001**, *31*, 983-995, https://doi.org/10.1081/SIM-100105255.
10. Ghosh, R.; Rahaman, S.H.; Lin, C.N.; Lu, T.H.; Ghosh, B.K. Coordination behaviour of symmetrical hexadentate N-donor Schiff bases towards zinc (II) pseudohalides: Syntheses, crystal structures and luminescence. *Polyhedron* **2006**, *25*, 3104-3112, https://doi.org/10.1016/j.poly.2006.05.037.
11. Chandrasekhar, S.; Reddy, C.R.; Babu, B.N. Rapid defunctionalization of carbonyl group to methylene with polymethylhydrosiloxane− B (C6F5) 3. *The Journal of Organic Chemistry* **2002**, *67*, 9080-9082, https://doi.org/10.1021/jo0204045.
12. Macías, B.; Villa, M.V.; Gómez, B.; Borrás, J.; Alzuet, G.; González-Álvarez, M.; Castiñeiras, A. DNA interaction of new copper (II) complexes with sulfonamides as ligands. *Journal of Inorganic Biochemistry* **2007**, *101*, 444-451, https://doi.org/10.1016/j.jinorgbio.2006.11.007.
13. Bedford, R.B.; Huwe, M.; Wilkinson, M.C. Iron-catalysed Negishi coupling of benzyl halides and phosphates. *Chemical Communications* **2009**, *5*, 600-602, https://doi.org/10.1039/B818961G.

14. Tanaka, K.; Shimoura, R.; Caira, M.R. Synthesis, crystal structures and photochromic properties of novel chiral Schiff base macrocycles. *Tetrahedron Letters* **2010**, *51*, 449-452.15, https://doi.org/10.1016/j.tetlet.2009.11.062.
15. Yahsi, Y.; Gungor, E.; Kazak, C.; Kara, H. Crystal structure of a μ-oxo-bridged dimeric iron (III) complex. *Journal of Structural Chemistry* **2015**, *56*, 1540-1544, https://doi.org/10.1134/S0022476615080120.
16. Shabani, F.; Saghatforoush, L.A.; Ghammamy, S. Synthesis, characterization and anti-tumour activity of Iron (III) Schiff base complexes with unsymmetric tetradentate ligands. *Bulletin of the Chemical society of Ethiopia* **2010**, *24*, 193-199, https://doi.org/10.4314/bcse.v24i2.54741.
17. McDonald, A.R.; Que, J.L. High-valent nonheme iron-oxo complexes: Synthesis, structure, and spectroscopy. *Coordination Chemistry Reviews* **2013**, *257*, 414-428, https://doi.org/10.1016/j.ccr.2012.08.002.
18. Rowland, J.M.; Olmstead, M.; Mascharak, P.K. Syntheses, structures, and reactivity of low spin iron (III) complexes containing a single carboxamido nitrogen in a [FeN5L] chromophore. *Inorganic Chemistry* **2001**, *40*, 2810-2817, https://doi.org/10.1021/ic001127s.
19. Mascharak, P.K. The Active Site of Nitrile Hydratase: An Assembly of Unusual Coordination Features by Nature. In: *Molecular Design in Inorganic Biochemistry. Structure and Bonding*. Rabinovich, D. (eds), Volume 160, Springer, Berlin, Heidelberg. **2013**; https://doi.org/10.1007/430_2012_85.
20. Burger, R.M. Nature of Activated Bleomycin. In: *Metal-Oxo and Metal-Peroxo Species in Catalytic Oxidations. Structure and Bonding*. Meunier, B. (eds), Volume 97, Springer, Berlin, Heidelberg. **2001**; https://doi.org/10.1007/3-540-46592-8_10.
21. Canali, L.; Sherrington, D.C. Utilisation of homogeneous and supported chiral metal (salen) complexes in asymmetric catalysis. *Chemical Society Reviews* **1999**, *28*, 85-93, https://doi.org/10.1039/A806483K.
22. Rahman, L.A.; Abu-Dief, A.M.; Hashem, N.A.; Seleem, A.A. Recent advances in synthesis, characterization and biological activity of nano sized Schiff base amino acid M (II) complexes. *International Journal of Nano Chemistry* **2015**, *1*, 79-95.
23. Dianu, M.L.; Kriza, A.; Stanica, N.; Musuc, A.M. Transition metal M (II) complexes with isonicotinic acid 2-(9-anthrylmethylene)-hydrazide. *Journal of Serbian Chemical Society* **2010**, *75*, 1515-1531, https://doi.org/10.2298/JSC091113121D.
24. Subbiah, A.; Sambamoorthy, S. Synthesis, Characterization, Fluorescence, Electrochemical, Antimicrobial and Cytotoxic studies of Cobalt (II), Nickel (II) and Copper (II) complexes with N-4-Methylphenyl (2, 4-dihydroxy acetophenylideneimine). *Oriental Journal of Chemistry* **2018**, *34*, 2008-2016, http://dx.doi.org/10.13005/ojc/3404039.
25. Dias, I.M.; Junior, H.C.; Costa, S.C.; Cardoso, C.M.; Cruz, A.G.; Santos, C.E.; Candela, D.R.; Soriano, S.; Marques, M.M.; Ferreira, G.B.; Guedes, G.P. Mononuclear coordination compounds containing a pyrazole-based ligand: Syntheses, magnetism and acetylcholinesterase inhibition assays. *Journal of Molecular Structure* **2020**, *1205*, http://dx.doi.org/10.1016/j.molstruc.2019.127564.
26. Wei, Z.L.; Wang, L.; Wang, J.F.; Guo, W.T.; Zhang, Y.; Dong, W.K. Two highly sensitive and efficient salamo-like copper (II) complex probes for recognition of CN−. *Spectrochimica Acta Part A: Molecular and Biomolecular Spectroscopy* **2020**, *228*, http://dx.doi.org/10.1016/j.saa.2019.117775.
27. Dkhil, M.A.; Zreiq, R.; Hafiz, T.A.; Mubaraki, M.A.; Sulaiman, S.; Algahtani, F.; Abdel-Gaber, R.; Al-Shaebi, E.M.; Al-Quraishy, S. Anthelmintic and antimicrobial activity of Indigofera oblongifolia leaf extracts. *Saudi Journal of Biological Sciences* **2020**, *27*, 594-598, https://doi.org/10.1016/j.sjbs.2019.11.033.
28. Yeşilyurt, N.; Yılmaz, B.; Ağagündüz, D.; Capasso, R. Involvement of probiotics and postbiotics in the immune system modulation. *Biologics* **2021**, *1*, 89-110, https://doi.org/10.3390/biologics1020006.
29. Kumar, K.N.; Amperayani, K.R.; Parimi, U.D. Synthesis and Antimicrobial activity of Piperazine analogues containing [1, 3, 4] Thiadiazole ring. *Research Journal of Pharmacy and Technology* **2021**, *14*, 4710-4714, https://doi.org/10.52711/0974-360X.2021.00819.
30. Brar, R.K.; Jyoti, U.; Patil, R.K.; Patil, H.C. Fluoroquinolone antibiotics: An overview. *Adesh University Journal of Medical Sciences & Research* **2020**, *2*, 26-30, https://doi.org/10.25259/AUJMSR_12_2020.
31. Chen, X.; Dou, Q.P., Liu, J. and Tang, D. Targeting Ubiquitin–Proteasome System with Copper Complexes for Cancer Therapy. *Frontiers in Molecular Biosciences* **2021**, *8*, https://doi.org/10.3389/fmolb.2021.649151.
32. Baran, E.J. Oxovanadium (IV) and oxovanadium (V) complexes relevant to biological systems. *Journal of Inorganic Biochemistry* **2000**, *80*, 1-10, https://doi.org/10.1016/s0162-0134(00)00032-5.
33. Jovanovski, G.; Tančeva, S.; Šoptrajanov, B. The SO2 stretching vibrations in some metal saccharinates: spectra-structure correlations. *Spectroscopy Letters* **1995**, *28*, 1095-1109, https://doi.org/10.1080/00387019508009449.
34. Enamullah, M.; Zaman, M.A.M.; Bindu, M.M.; Islam, M.K.; Islam, M.A. Experimental and theoretical studies on isatin-Schiff bases and their copper (II)-complexes: Syntheses, spectroscopy, tautomerism, redox potentials, EPR, PXRD and DFT/TDDFT. *Journal of Molecular Structure* **2020**, *1201*, https://doi.org/10.1016/j.molstruc.2019.127207.
35. Lange, A.; Mills, R.E.; Lange, C.J.; Stewart, M.; Devine, S.E.; Corbett, A.H. Classical nuclear localization signals: definition, function, and interaction with importin α. *Journal of Biological Chemistry* **2007**, *282*, 5101-5105, https://doi.org/10.1074/jbc.R600026200.

36. de Oliveira Silva, D. Ruthenium Compounds Targeting Cancer Therapy. In: *Frontiers in Anti-cancer Drug Discovery*. Bentham Science Publisher **2014**; https://doi.org/10.2174/9781608592251140401.
37. Tripathi, L.; Kumar, P.; Singhai, A.K. Role of chelates in treatment of cancer. *Indian Journal of Cancer* **2007**, *44*, 62-71, https://doi.org/10.4103/0019-509x.35813.
38. Elo, H. The antiproliferative agents trans-bis (resorcylaldoximato) copper (II) and trans-bis (2, 3, 4-trihydroxybenzaldoximato) copper (II) and cytopathic effects of HIV. *Zeitschrift für Naturforschung C* **2004**, *59*, 609-611, https://doi.org/10.1515/znc-2004-7-828.
39. Singh, M.K.; Bhaumik, S.K.; Karmakar, S.; Paul, J.; Sawoo, S.; Majumder, H.K.; Roy, A. Copper salisylaldoxime (CuSAL) imparts protective efficacy against visceral leishmaniasis by targeting Leishmania donovani topoisomerase IB. *Experimental Parasitology* **2017**, *175*, 8-20, https://doi.org/10.1016/j.exppara.2017.02.010.
40. Mallick, S.; Mondal, S.; Bera, B.K.; Karmakar, P.; Moi, S.C.; Ghosh, A.K. Kinetics and mechanism of the ligand substitution reaction of di-μ-hydroxobis (bipyridyl) dipalladium (II) ion with thiourea in aqueous solution. *Transition Metal Chemistry* **2010**, *35*, 469-475, https://doi.org/10.1007/s11243-010-9351-4.
41. Wehbe, M.; Leung, A.W.; Abrams, M.J.; Orvig, C.; Bally, M.B. A Perspective–can copper complexes be developed as a novel class of therapeutics? *Dalton Transactions* **2017**, *46*, 10758-10773, https://doi.org/10.1039/C7DT01955F.
42. Kim, Y.; Lee, J.; Son, Y.H.; Choi, S.U.; Alam, M.; Park, S. Novel nickel (II), palladium (II), and platinum (II) complexes having a pyrrolyl-iminophosphine (PNN) pincer: Synthesis, crystal structures, and cytotoxic activity. *Journal of Inorganic Biochemistry* **2020**, *205*, https://doi.org/10.1016/j.jinorgbio.2020.111015.
43. Yadav, S. Potential of Metal Complexes for the Treatment of Cancer: Current Update and Future Prospective. *Chemistry of Biologically Potent Natural Products and Synthetic Compounds* **2021**, *1*, 183-204, https://doi.org/10.1002/9781119640929.ch7.
44. Alhasan, D.A. In Vitro Antimicrobial Activity of Curcumin-Copper Complex. *University of Thi-Qar Journal* **2021**, *16*, 73-97.
45. Tisato, F.; Marzano, C.; Porchia, M.; Pellei, M.; Santini, C. Copper in diseases and treatments, and copper-based anticancer strategies. *Medicinal Research Reviews* **2010**, *30*, 708-749, https://doi.org/10.1002/med.20174.
46. Pérez-Rebolledo, A.; Teixeira, L.R.; Batista, A.A.; Mangrich, A.S.; Aguirre, G.; Cerecetto, H.; González, M.; Hernández, P.; Ferreira, A.M.; Speziali, N.L.; Beraldo, H. 4-Nitroacetophenone-derived thiosemicarbazones and their copper (II) complexes with significant in vitro anti-trypanosomal activity. *European Journal of Medicinal Chemistry* **2008**, *43*, 939-948, https://doi.org/10.1016/j.ejmech.2007.06.020.
47. Xiao, Y.; Wang, Q.; Huang, Y.; Ma, X.; Xiong, X.; Li, H. Synthesis, structure, and biological evaluation of a copper (II) complex with fleroxacin and 1, 10-phenanthroline. *Dalton Transactions* **2016**, *45*, 10928-10935, https://doi.org/10.1039/C6DT00915H.
48. Sharma, S.; Athar, F.; Maurya, M.R.; Azam, A. Copper (II) complexes with substituted thiosemicarbazones of thiophene-2-carboxaldehyde: synthesis, characterization and antiamoebic activity against E. histolytica. *European Journal of Medicinal Chemistry* **2005**, *40*, 1414-1419, https://doi.org/10.1016/j.ejmech.2005.05.013.
49. Iakovidis, I.; Delimaris, I.; Piperakis, S.M. Copper and its complexes in medicine: a biochemical approach. *Molecular Biology International* **2011**, *2011*, https://doi.org/10.4061/2011/594529.
50. Tabrizi, L.; Chiniforoshan, H. Synthesis and C–H activation reactions of cyclometalated copper (i) complexes with NCN pincer and 1, 3, 5-triaza-7-phosphaadamantane derivatives: in vitro antimicrobial and cytotoxic activity. *New Journal of Chemistry* **2017**, *41*, 10972-10984, https://doi.org/10.1039/C7NJ02500A.
51. Kimmatkar, N.; Thawani, V.; Hingorani, L.; Khiyani, R. Efficacy and tolerability of Boswellia serrata extract in treatment of osteoarthritis of knee–a randomized double blind placebo controlled trial. *Phytomedicine* **2003**, *10*, 3-7, https://doi.org/10.1078/094471103321648593.
52. Silvestri, A.; Barone, G.; Ruisi, G.; Anselmo, D.; Riela, S.; Liveri, V.T. The interaction of native DNA with Zn (II) and Cu (II) complexes of 5-triethyl ammonium methyl salicylidene orto-phenylendiimine. *Journal of Inorganic Biochemistry* **2007**, *101*, 841-848, https://doi.org/10.1016/j.jinorgbio.2007.01.017.
53. Wu, J.Z.; Yuan, L.; Wu, J.F. Synthesis and DNA binding of μ-[2, 9-bis (2-imidazo [4, 5-f][1, 10] phenanthroline)-1, 10-phenanthroline] bis [1, 10-phenanthrolinecopper (II)]. *Journal of Inorganic Biochemistry* **2005**, *99*, 2211-2216, https://doi.org/10.1016/j.jinorgbio.2005.08.002.
54. Efthimiadou, E.K.; Thomadaki, H.; Sanakis, Y.; Raptopoulou, C.P.; Katsaros, N.; Scorilas, A.; Karaliota, A.; Psomas, G. Structure and biological properties of the copper (II) complex with the quinolone antibacterial drug N-propyl-norfloxacin and 2, 2′-bipyridine. *Journal of Inorganic Biochemistry* **2007**, *101*, 64-73, https://doi.org/10.1016/j.jinorgbio.2006.07.019.
55. Efthimiadou, E.K.; Karaliota, A.; Psomas, G. Structure, antimicrobial activity and DNA-binding properties of the cobalt (II)–sparfloxacin complex. *Bioorganic & Medicinal Chemistry Letters* **2008**, *18*, 4033-4037, https://doi.org/10.1016/j.bmcl.2008.05.115.
56. Katsarou, M.E.; Efthimiadou, E.K.; Psomas, G.; Karaliota, A.; Vourloumis, D. Novel copper (II) complex of N-propyl-norfloxacin and 1, 10-phenanthroline with enhanced antileukemic and DNA nuclease activities. *Journal of Medicinal Chemistry* **2008**, *51*, 470-478, https://doi.org/10.1021/jm7013259.

57. Lauro, F.V.; Francisco, D.C.; Marcela, R.N.; Virginia, M.A.; Patricia, H.V.; Laura, B.C.; Eduardo, P.G.; Maria, L.R.; Hau Heredia, Lenin.; Tomas, L.G.; Regina, C.C.; Yaritza, B.B. Synthesis and theoretical analysis of interaction from an adamantane-steroid derivative with both COX-1 and COX-2. *Biointerface Research in Applied Chemistry* **2019**, *9*, 3860-3865, https://doi.org/10.33263/BRIAC92.860865.
58. Abaszadeh, M.; Sheibani, H.; Mola, A. Theoretical and experimental investigations into the structural, electronic, and molecular properties of 1,5-dihydropyrano 2,3-c chromene derivatives. *Biointerface Research in Applied Chemistry* **2020**, *10*, 5586-5591, https://doi.org/10.33263/BRIAC103.586591.
59. Drapak, I.; Foliush, V.; Chaban, T.; Matiychuk, V. Synthesis antimicrobial and antitumor activities of 2- 5-(2-R-benzyl)thiazol-2-ylimino thiazolidin-4-ones. *Biointerface Research in Applied Chemistry* **2020**, *10*, 5507-5511, https://doi.org/10.33263/BRIAC103.507511.
60. Fadda, A.A.; Mohammed, A.R.; Abdel-Galil, E. Synthesis and antimicrobial evaluation of some 4-quinolinylazo-N-pyrimidinyl benzenesulfonamide derivatives. *Biointerface Research in Applied Chemistry* **2020**, *10*, 4846-4852, https://doi.org/10.33263/briac101.846852.
61. Kendrekar, P.; Mashele, S.; Tekale, S.; Pawar, R. Synthesis of Some Novel and Potent Anti-Plasmodial Aminoalkyl Chalcone Derivatives. *Biointerface Research in Applied Chemistry* **2020**, *10*, 6076-6081, https://doi.org/10.33263/briac105.60766081.
62. Konovalova, S.; Avdeenko, A.; Baranovych, D.; Lubenets, V. Synthesis and Bioactivity of Quinone Mono- and Dioxime Salts. *Biointerface Research in Applied Chemistry* **2020**, *10*, 6148-6156, https://doi.org/10.33263/briac105.61486156.
63. Konovalova, S.; Avdeenko, A.; Lubenets, V.; Novikov, V. Synthesis and bioactivity of benzohydrazide derivatives. *Biointerface Research in Applied Chemistry* **2020**, *10*, 5797-5802, https://doi.org/10.33263/briac104.797802.
64. Alorini, T.A.; Al-Hakimi, A.N.; Saeed, S.E.S.; Alhamzi, E.H.L.; Albadri, A.E. Synthesis, characterization, and anticancer activity of some metal complexes with a new Schiff base ligand. *Arabian Journal of Chemistry* **2022**, *15*, https://doi.org/10.1016/j.arabjc.2021.103559.
65. Gaurav, S.; Sujata, B.; Vijay, C.; Amit, K.; Asiri, A.M.; Alamry, K.A. Chemical modification of raw Quercus leucotricophora wood strips and studies of its physicochemical properties and antifungal behavior. *Desalination and Water Treatment* **2019,** *150*, 252-262, https://doi.org/10.5004/dwt.2019.23696.
66. Ibrahim, G.P.S.; Isloor, A.M.; Asiri, A.M.; Farnood, R. Tuning the surface properties of Fe_3O_4 by zwitterionic sulfobetaine: application to antifouling and dye removal membrane. *International Journal of Environmental Science and Technology* **2020**, *17*, 4047-4060, https://doi.org/10.1007/s13762-020-02730-z.